



Conjugate Effect on the Thermal Characteristics of Air Impinging Jet

Ghassan Nasif^{1,2}, Yasser El-Okda^{2,*}

¹ Department of Mechanical, Automotive, and Materials Engineering, University of Windsor, ON, Canada

² Mechanical Engineering Department, Higher Colleges of Technology, Abu Dhabi Men's College, Abu Dhabi, UAE

ARTICLE INFO

Article history:

Received 23 June 2021

Received in revised form 13 September 2021

Accepted 14 September 2021

Available online 31 October 2021

Keywords:

CFD simulation; Conjugate heat transfer; Nusselt number; jet impingement; turbulent model

ABSTRACT

A computational fluid dynamics (CFD) investigation to determine the conjugate heat transfer (CHT) effect on the stagnation and local thermal characteristics due to an impinging process has been carried out in this study using STAR-CCM+ - Siemens PLM commercial code. The transient Navier-Stokes's equations are numerically solved using a finite volume approach with $k-\omega$ SST eddy viscosity as the turbulence model. A fully developed circular air jet with different Reynolds numbers, impinging vertically onto a heated flat disc with different metals, thicknesses, and boundary heat fluxes are employed in the current study to examine the thermal characteristics and provide an enhanced picture for the convection mechanism that used in jet cooling technology. It is found that the thermal characteristics are influenced by the thermal conductivity and thickness of the target upon using air as a cooling jet. The CHT process enhances the local convective heat transfer at the fluid-solid interface due to the variation in transverse and axial conductive heat transfer inside the metal up to a certain radial extent from the stagnation region compared to the process with no CHT. The extent of the radial enhancement depends on the thermal conductivity of the metal. For a given thermal conductivity, the CHT process acts to increase the temperature and convective heat flux of the stagnation region as the metal thickness increases.

1. Introduction

Impinging jets provide an effective means to transfer energy or mass in many industrial applications. A directed liquid or gaseous flow released against a surface can easily transfer large amounts of thermal energy between the impingement target and the fluid. Jet impingement is characterized by very low thermal resistance and is relatively simple to implement. In many applications, the conventional cooling requirements are limited by other restrictive factors such as available space, coolant selection, local environmental conditions, and maximum allowable surface temperature. All these restrictions can be eliminated by using jet cooling technology.

Nasif *et al.*, [1-3], Steven and Webb [4], Lee and Lee [5], and Liu *et al.*, [6] have extensively studied the thermal and flow characteristics associated with liquid jets impinging on surfaces. These studies are in relatively good agreement with one another. The maximum heat transfer coefficient (HTC) due

* Corresponding author.

E-mail address: yelokda@hct.ac.ae (Yasser El-Okda)

to the jet impingement occurs in a small region around the stagnation region [3]. Nasif *et al.*, [1] have used CFD simulations to show that for a given Reynolds number, the temperature distribution on the impinging surface will be more uniform for larger nozzles compared to smaller nozzles. Smaller nozzles provide more efficient convective cooling in the region around the stagnation region, while the larger nozzles cool the surface more uniformly. Experiments were performed by Liu *et al.*, [6] to study the characteristics of an impinging turbulent jet onto a fixed surface subjected to constant heat flux, using different nozzle diameters and a wide range of Reynolds numbers. The investigations showed an obvious dependence of the stagnation zone Nusselt number on Reynolds number, Prandtl number, and velocity gradient and less dependency on the nozzle to plate spacing. Haidar *et al.*, [7] carried out an experimental and numerical study of the heat transfers in a rotating disk with an impinging jet. The disk is cooled using the impingement of an eccentric air jet. They revealed that for a fixed jet Reynolds number, the local Nusselt number is increasing compared to the fixed disc and it was a function of rotational velocity and radius of the disc. The effect of adding air into water jet flow for heat transfer enhancement was investigated for impinging jets by Aroonrujiphan & Nuntadusit [8]. It was found that the volumetric fraction of 0.2 gave the maximum heat transfer enhancement of about 33% compared to the case of the water jet. Furthermore, the increase of volumetric fraction in the range between 0.2 - 0.7 will act to decrease the average Nusselt number.

Zhu *et al.*, [9] investigated the wall effect on the HTC of an impinging jet. They concluded that the conjugate heat transfer (CHT) approach redistributes the boundary heat flux and changes it from a uniform heat flux boundary to a nearly isothermal boundary. The heat redistribution is also driven by the non-uniform distribution of the HTC on the impinged surface. The degree of heat redistribution is related to both conductive thermal resistance in the solid and convective thermal resistance at the interface. The study also revealed that the CHT prediction may have a negative impact on the local Nusselt number (Nu), indicating a decrease in the local Nu as the thermal conductivity of the solid decreases. Bouafia *et al.*, [10] performed a numerical study to evaluate the effect of the CHT on heat transfer. In this study, the problem of conjugate natural convection in a square porous cavity saturated with Al₂O₃/H₂O in the presence of two isothermal cylindrical sources was investigated numerically. The results show that the average Nusselt number increases when the conductivity ratio raises. Furthermore, the heat exchange reduces with the increase in the solid portion thickness, but it becomes constant for the thick wall at a higher value of thermal conductivity ratio. Mensch & Thole [11] used a conjugate heat transfer approach to account for the combined effects of both internal and external cooling. The geometry that was employed in the latter study is a turbine blade endwall that includes impingement, film cooling, and heat conduction through the endwall. The conclusion from this study revealed that the internal HTC of impingement geometries is sensitive to geometric parameters, while the average temperature of the endwall external surface is not particularly sensitive to geometric parameters. Hussien *et al.*, [12] investigated the entropy generation due to the conjugate heat transfer process in a porous cavity. Three different cavities with finite walls thickness and heat source locations are considered in their study. They revealed that the strength of the fluid flow and the convection heat transfer is directly proportional to Rayleigh number (Ra), thermal conductivity (κ), thermal source length, and cavity aspect ratio (AR), while they are inversely proportional to cavity walls thickness.

In all previous studies, the effects of the nozzle size, jet Reynolds number, nozzle-to-target distance, and working fluids on the thermal characteristics were extensively investigated. However, the conjugate effect has not been adequately addressed in these studies. The CHT model was developed after computers came into wide use to substitute the empirical relation of proportionality of heat flux to temperature difference with heat transfer coefficient. Conjugate heat transfer is a crucial issue in many engineering problems, which can be examined in different ways. Analytical

approaches generate good results to identify the main parameters of the problem and to verify the codes. However, the applications of the analytical methods are restricted to very simple configurations [13-15]. Experiments, which are an alternative approach to the analytical methods, are considerably expensive and cannot be relied on in the industry. The modern computational CHT was developed after computers came into a broad application to replace the empirical expressions of proportionality of heat flux to temperature difference with heat transfer coefficient (HTC). The state-of-the-art of computational method involves coupling the conduction in the solid and convection in the fluid to predict the HTC at the interface. The coupled approach is more reliable and common than a decoupled solution [16]. In the computational CHT approach, two separate simulations are set up, one for fluid analysis and another for solid thermal analysis. Assuming the temperature distribution on the wall boundary, the fluid flow problem is solved to determine the local HTC distribution on the wall. The HTC distribution with the reference temperature is applied to the solid thermal simulation to re-evaluate the temperature distribution in the solid. The wall temperature distribution predicted by the solid thermal analysis is fed back to the transient flow simulation and applied as a wall boundary condition to re-evaluate the modified HTC distribution at the interface. The iteration process continues until the solution is obtained with suitable accuracy.

The objective of this study is to numerically investigate the effect of the conjugate heat transfer method on the problem thermal characteristic due to an impinging jet process. For this end, CFD simulations of fully-developed circular air jets impinging orthogonally on a heated flat disc with different heat fluxes and thicknesses of 0.0, 5.0, and 10.0 mm are employed in the present study. The thermal characteristics, i.e., local and stagnation Nusselt numbers, temperature profile, convective heat transfer, etc., are compared for the different cases in this investigation.

2. Methodology

Figure 1 shows the computational domain with relevant boundary conditions. The cases are simulated using STAR-CCM+ - Siemens PLM commercial code with an unstructured polyhedral mesh. The major advantage of polyhedral cells is that they generally have many neighbours, so gradients of the variable at cell centres can be much better approximated compared to other mesh types. Polyhedrons are also less sensitive to stretching than other mesh types, i.e., tetrahedrons, which results in better mesh quality leading to improved numerical stability of the model. In addition, numerical diffusion is reduced due to mass exchange over numerous faces. This leads to a more accurate solution achieved with a lower cell count [17]. The solid part in the computational domain is created by extruding the interface to a certain thickness (for the CHT simulations) as shown in Figure 1. The governing equations for transient analysis include continuity, momentum, and energy equations. Each of these equations can be described in a general way by the transport of a particular scalar quantity ϕ , represented in a continuous integral form as [18-20]

$$\frac{\partial}{\partial t} \int_{CV} \rho \phi dV + \oint_A \mathbf{n} \cdot (\rho \phi \mathbf{u}) dA = \oint_A \mathbf{n} \cdot (\Gamma_{\phi} \nabla \phi) dA + \int_{CV} S_{\phi} dV \quad (1)$$

where CV is the control volume, A is the surface area of the control volume, \mathbf{n} is the unit outward normal vector to the surface element dA , \mathbf{u} is the velocity vector and ρ is the density. The terms in Eq. (1), from left to right are, the rate of change the property ϕ in the control volume, the rate of change the property ϕ due to the convection flux across the boundaries of the control volume, the rate of change the property ϕ due to the diffusive flux across the boundaries of the control volume, and the source term. The source term in Eq. (1) contains the effects of the pressure gradient and all types of body forces. The set of transport equations is obtained by selecting appropriate expressions

for the diffusion coefficient Γ_ϕ and source term S_ϕ and setting the variable ϕ in Eq. (1) to velocity vector components for momentum equations, and i for energy equation, where i is the internal energy of the fluid or solid. The integral form of the mass conservation equation can also be obtained from Eq. (1) by setting $\phi = 1$ and the source term $S_\phi = 0$.

Grids independent study was carried out in the earlier stage to select the optimum mesh count. The criteria for choosing the cell count in the current study are based on the validation process, i.e., the numerical results for many grids and many parameter settings were checked and compared with experimental results. Prism layers are clustered at the jet trajectory and the fluid-solid interface to better resolve the wall effect, producing a dimensionless wall distance value of $y^+ < 3.0$ at the solid-fluid interface. First-order implicit time marching and second-order spatial differencing are used to discretize the governing equations, within a finite volume framework. The $k-\omega$ SST eddy viscosity model has been selected as the turbulent model in this study. The CHT is used to couple the heat transfer solution between fluid and solid. The time step for the simulations was set at 1×10^{-3} s with twenty internal iterations. Pipe nozzle sizes of $d = 25.0$ mm, with nozzle-to-target distance $h/d = 6.0$ and various bulk velocities at 20°C , are used in the study. The fully-developed velocity profile at the nozzle exit is extracted from a separate simulation and mapped at the nozzle exit as shown in Figure 1 to ensure a fully developed velocity profile, pipes with a length to diameter ratio of $L/d = 50$ are used in separate simulations. The effect of the conjugate heat transfer (CHT) is investigated by using three different materials, i.e., copper (Cu), aluminium (Al), and stainless steel (316SST). The thermal properties of these materials are given in Table 1. Two plate thicknesses (t_p) are used in the study, i.e., 5.0 mm and 10.0 mm while different heat fluxes are employed in the simulations as a thermal boundary. The heat fluxes (q_B) between 500 and 5000 W/m^2 are used as thermal boundary conditions in this study and are applied at the bottom of the disc in Figure 1. The subscripts (B) and (T) will be used in this study to represent the heat fluxes at the bottom (constant heat flux boundary) and the top (convective heat flux at the interface) surfaces of the plate, respectively. The computational results of the CHT simulations are compared with each other and with the computational results from the jet impingement with no CHT, i.e., plate with zero thickness, to investigate the conjugate effect on the HTC. In the current study, the computational results are considered to have converged when the continuity, momentum, and energy scaled residuals fall below 10^{-6} .

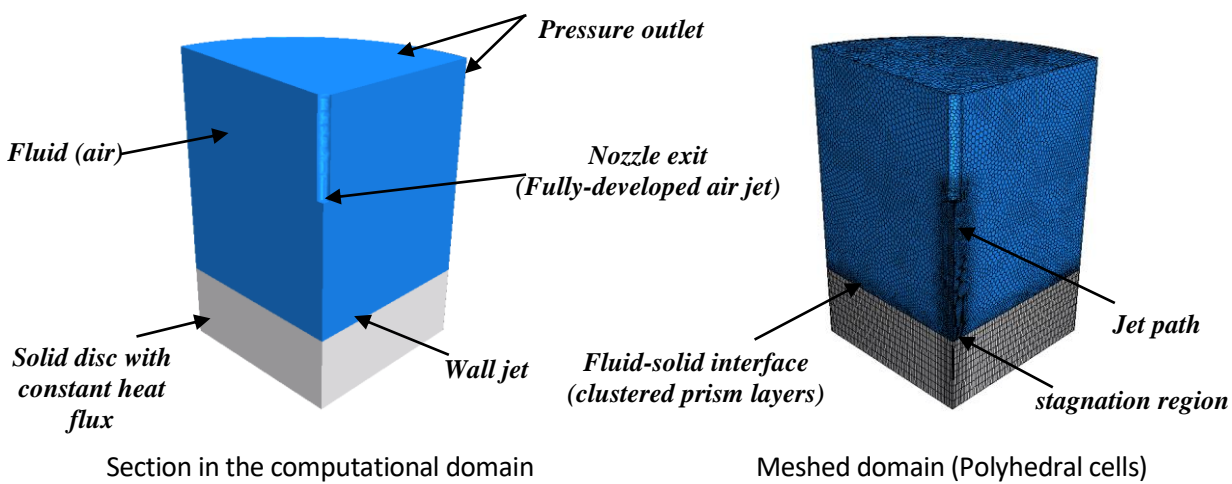


Fig. 1. Computational domain with relevant boundary conditions

Table 1
 Physical properties of the investigated metals

	Density ρ (kg/m ³)	Thermal Conductivity κ (W/m. K)	Specific Heat c_p (J/kg. K)	Thermal Diffusivity α (m ² /s)
Copper (Cu)	8940	398	386	1.2E-04
Aluminum (Al)	2702	237	903	1.0E-04
Stainless Steel (316 SST)	7990	15.4	500	4.0E-06

3. Validation

The normalized local Nusselt number from the numerical simulations is compared with experimental data [5] at different radial locations (r) from the stagnation region as shown in Figure 2. In this figure, the Nu_0 and Nu represent the stagnation region and local Nusselt number, respectively. The local Nusselt number (Nu) is normalized using the stagnation Nusselt number (Nu_0), while the radial direction is normalized by the diameter of the nozzle. The Nusselt number is calculated based on the nozzle diameter and the air temperature at the nozzle exit, i.e., 20 °C. Three jet Reynolds numbers for nozzle diameter of $d = 25.0$ mm and $h/d = 6.0$ are used in the validation process, i.e., $Re = 5000$, 15000 and 30000 . The validation process is performed by neglecting the conjugate effect to mimic the experiment setup [5], i.e., the jet impinges a flat plate with zero thickness and $q_B = 1000$ W/m². The difference between the computational and experimental results increases with the Reynolds number. It is shown that the computational model can reproduce the experimental data with a maximum difference of less than 10% for $Re = 30000$. Therefore, the present simulations can satisfactorily predict the heat transfer performance of the impinging jet. The validation process was also performed for $h/d = 4.0$ and 10.0 ; the results were comparable to what is shown in Figure 2.

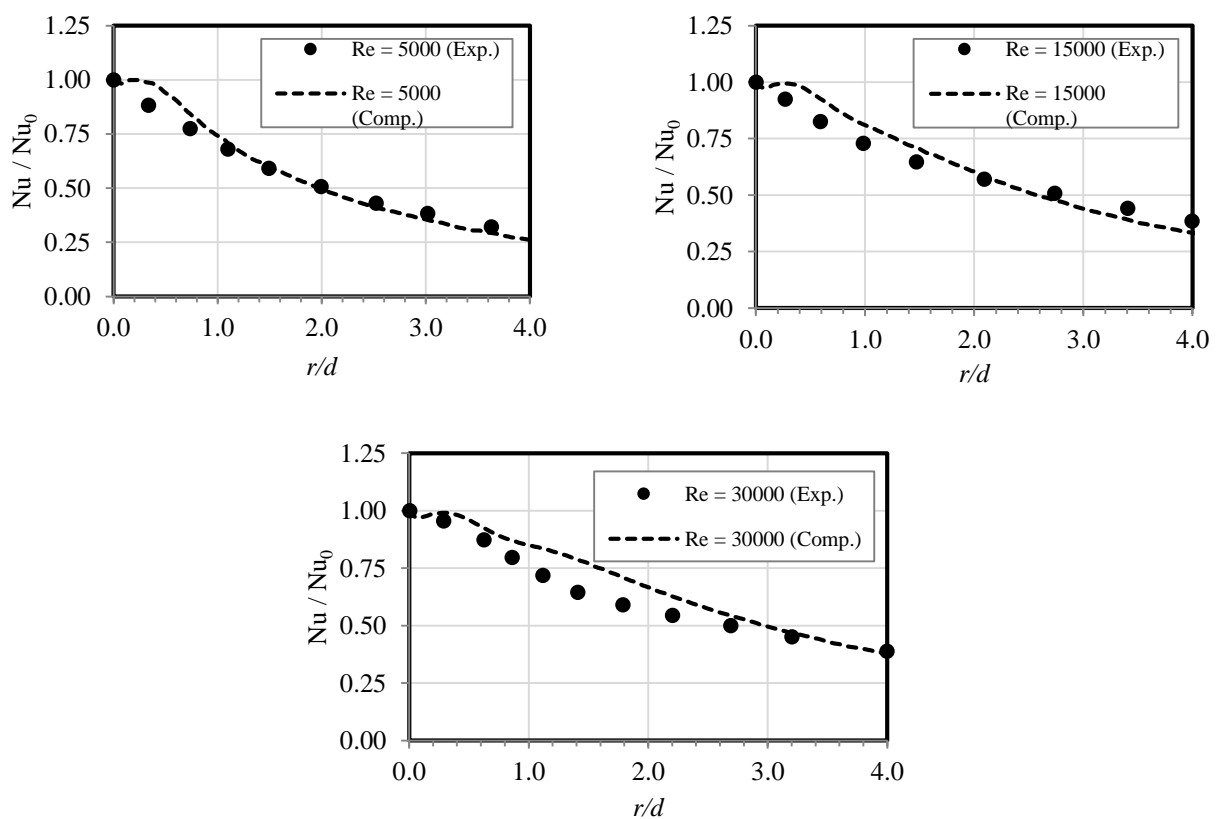


Fig. 2. Comparison between computational and experimental results at $h/d = 6.0$

4. Results

In this section, the jet Reynolds number of $Re = 20000$ and nozzle-to-target distance at $h/d = 6.0$ are used as sample operating condition to present the results. The case of no CHT process is used as the benchmark to evaluate the relative thermal performance of various conjugate scenarios. When the solid plate has a finite thickness, the conductive heat transfer inside the solid influences the convective heat transfer from the plate surface. The CHT process will act to redistribute the uniform boundary heat flux inside the solid and make a difference not only at stagnation but also in the local Nusselt number. As the plate thickness (t_p) increases, the thermal resistance (R) in the radial direction ($R_r \propto 1/\kappa \cdot t_p$) decreases, while the thermal resistance in the axial direction ($R_a \propto t_p/\kappa$) increases. Here, the subscripts r and a represent the radial and axial directions, respectively. Therefore, the conductive heat transfer in the radial direction towards the impingement region, which acts as a heat sink, increases with the plate thickness, while the axial conductive heat transfer towards the surface (interface) decreases as the plate thickness increases. The boundary heat flux will not remain uniform at the interface as in the case of plate with zero thickness due to the conjugate effect. In the convective heat transfer problem that involves a CHT process, the HTC profile at the interface depends on the thermal properties and thickness of the plate besides the other flow parameters. Figure 3 shows the conjugate effect on the normalized local Nusselt number (Nu/Nu_0) profile of the jet impingement process. In this figure, two heat fluxes of $q_B = 1000$ & 1500 W/m^2 are used as a thermal boundary condition to present the results. For all disc materials that were used in the simulation (see Table 1), the Nu/Nu_0 profiles deviate downwards from the one with no CHT process as shown in Figure 3(a). The thermal conductivity of the metal has an effect on the CHT process and subsequently on the normalized Nu/Nu_0 profile. The profile is shifted up towards the profile with no CHT as the metal thermal conductivity decreases (316SST). This can be attributed to that the radial and axial thermal resistances of metal with lower thermal conductivity approaches to the case of plate with zero thickness, i.e., ∞ and 0 , respectively. The value of the parameter ($1/\kappa \cdot t_p$) which influences the thermal resistance in the radial direction in 5.0 mm disc is 0.5, 0.85, and 13.0 K/W corresponding to Cu, Al, and 316SST, respectively. While the value of the parameter (t_p/κ) which impacts the thermal resistance in the axial direction in 5.0 mm disc is $1.25E-05$, $2.10E-05$, and $3.25E-04$ $m^2.K/W$ corresponding to Cu, Al, and 316SST, respectively. The effect of the disc thickness is presented in Figure 3(b). The conclusion that can be drawn from this figure is that the disc thickness has an insignificant effect on the Nu/Nu_0 distribution for the cases that are used in the current study with the air jet. The normalized Nusselt number profiles are comparable for Cu and Al metals due to their alike thermal characteristics as shown in Figure 3.

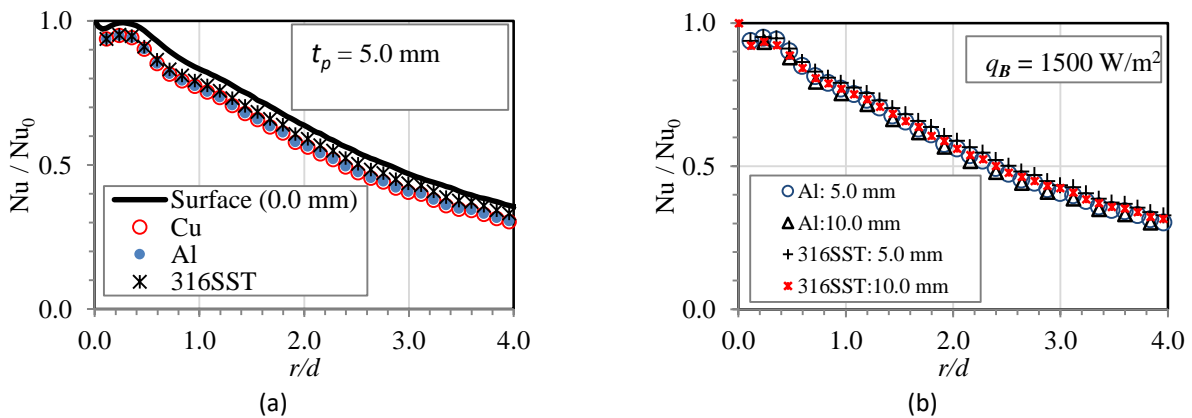


Fig. 3. The effect of (a) metal type, (b) metal thickness on the conjugate heat transfer (CHT)

In the current simulation, the effect of the thermal boundary condition and CHT on the Nu_0 have been investigated as shown in Figure 4. In this figure, three heat fluxes, i.e., $q_B = 500, 1000,$ and 1500 W/m^2 are used as a thermal boundary condition at the bottom surface of the disc. The fluxes at the bottom (q_B) and the convective fluxes at the top of the disc (q_T) are identical for jet impingement onto a plate with zero thickness, i.e., $q_B = q_T$. In jet impingement problems, the difference in the Nu_0 is more obvious at higher heat fluxes for the CHT process compared to plate with zero thickness. The stagnation Nusselt number is comparable for all metals when the boundary heat flux (q_B) is small, i.e., $q_B = 500 \text{ W/m}^2$. This indicates that CHT has a small influence on stagnation Nusselt number when the boundary heat flux value is small. The Nu_0 profile that implies a CHT process approaches the one with no CHT process as metal thermal conductivity decreases (316SST). Another observation that can be drawn from Figure 4 is that the Nu_0 decreases monotonically with the increase of the boundary heat flux in metals of high thermal conductivity (Al and Cu). This indicates that temperature at the stagnation region rises at a rate faster than the increase in the convective heat flux (q_{T0}) as the boundary heat flux (q_B), where q_{T0} is the convective heat flux at the stagnation point. The conjugate effect will enhance the energy flow towards the stagnation region and increase its temperature. Contrary to this, the Nu_0 slightly increases and becomes nearly steady at $q_B = 1000 \text{ W/m}^2$ with the increase of the boundary heat flux in metals with a low thermal conductivity as shown in Figure 4.

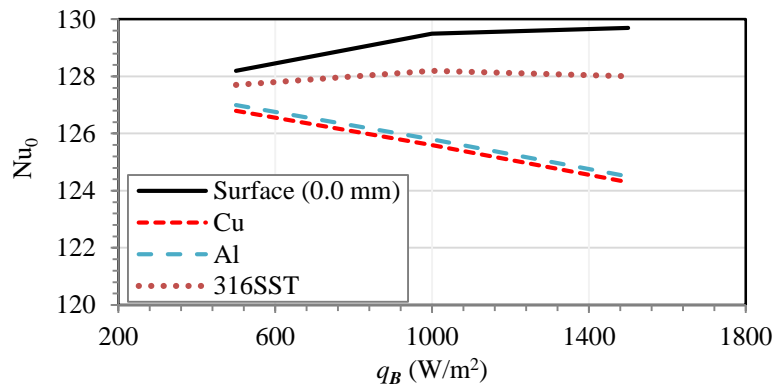


Fig. 4. The effect of the CHT process on stagnation region Nusselt number (Nu_0)

One of the CHT consequences is to enhance the conductive heat transfer in the radial direction towards the stagnation region. This is due to two combined effects: (i) reduction in the radial thermal resistance (R_r) of the solid, and (ii) increase in the axial thermal resistance (R_a) of the solid. Therefore, this will act to improve the local convective heat transfer at the stagnation region for all metals that used in the current investigation as shown in Figure 5. The degree of improvement depends on the thermal characteristics of the metal. In Figure 5, the local convective heat flux (q_T) at the top surface is given for the same operating conditions, i.e., $q_B = 1500 \text{ W/m}^2$ and $Re = 20000$, but different metals. The convective heat flux (q_T) profile becomes more uniform as $R_a \rightarrow \infty$, and more nonuniform as $R_a \rightarrow 0$ with distinct maxima at the stagnation region. The local convective heat transfer profile at the solid-fluid interface drops below the uniform profile with no CHT process at the transverse location of $r/d = 6.0$ in Al and Cu metals and $r/d = 8.0$ in 316SST metal as shown in Figure 5. This is attributed to the energy flow or diffusion to the stagnation region (see Table 1 for thermal diffusivity α) is comparable for Al and Cu metals. The thermal diffusivity of 316 SST is in order of 10^{-6} , while the thermal diffusivity of Al and Cu is in order of 10^{-4} . This will enhance the conductive heat flow towards the stagnation region, improve the convective heat transfer at locations $r/d < 6.0$, and attenuate it beyond $r/d = 6.0$ as in Al and Cu. Contrary to this, the conductive energy diffuses slower towards the stagnation region.

This will increase the axial conductive heat transfer compared to Al and Cu metal. Therefore, the local convective heat flux will be enhanced up to $r/d = 8.0$ in 316SST compared to no CHT process as shown in Figure 5.

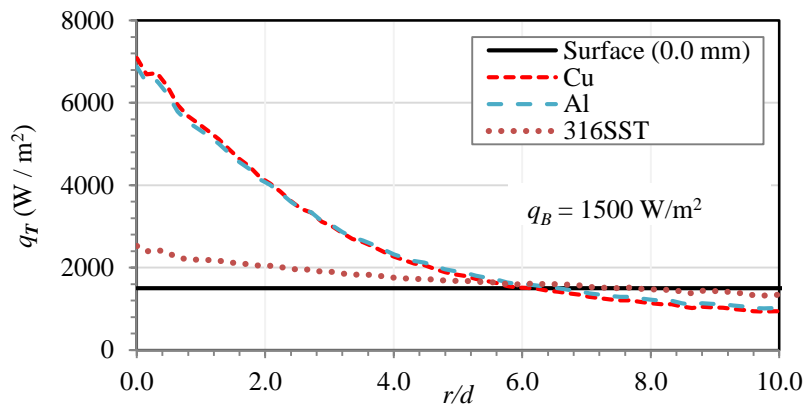


Fig. 5. The effect of the CHT process on local convective heat flux, $t_p = 5.0$ mm

The stagnation or the impingement region at the fluid-solid interface can be considered as a heat sink when it is at the disc side and as a heat source point when it is at the jet side. Generally, the CHT effect will act to decrease the conductive thermal resistance in the radial direction (R_r) and then enhances the energy flow towards the stagnation region for all metals that are used in this investigation. The amount of energy flow is proportional to the disc thickness and thermal conductivity of the metals. In metal with low thermal conductivity (316SST), the radial thermal resistance will decrease with the thickness faster than the increase of the axial thermal resistance. This will enhance the energy flow to the stagnation region as shown in Figure 6. In this figure, the q_{T0} represents the heat flux that is removed from the stagnation region. When the simulation reaches its steady state, i.e., the thermal characteristics are not changing with time, the amount of the conductive heat flux to the stagnation region equals the amount of convective heat flux that is eliminated by the air jet. The CHT effect will boost the heat drainage to/from the stagnation region as the disc thickness increases with 316SST metal. This is also the case for Al and Cu discs, however, the enhancement of energy flow with disc thickness seems to be less significant than the case of metal with low thermal conductivity (316SST) as shown in Figure 6. It is clearly shown in this figure that the thickness has less impact on q_{T0} for Cu and Al. The thickness impact becomes negligible as the metal thermal conductivity increases (case for Cu metal). Considering the above, one can conclude that for metal with low thermal conductivity, the thickness is more dominant than κ on thermal characteristics at the stagnation region, while κ is more dominant than the thickness on thermal characteristics for metal with high thermal conductivity. The influence of the thickness becomes negligible when the thermal conductivity of the metal approaches infinity.

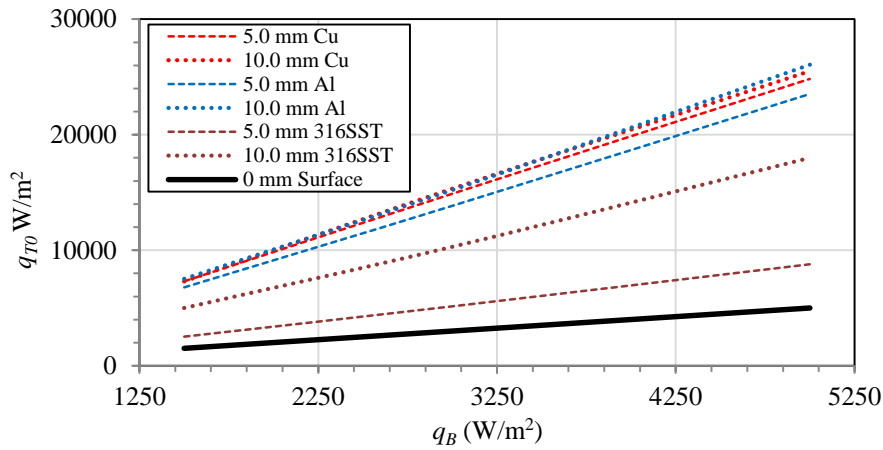


Fig. 6. Effect of the boundary heat flux (q_B) and CHT on the stagnation region convective heat flux (q_{T0})

The effect of the CHT process on the minimum disc temperature (T_{min}) is illustrated in Figure 7. In this figure, two thicknesses are used over a wide range of boundary heat flux (500 – 5000 W/m²) to investigate the combined effect of thermal boundary and CHT process on the T_{min} . The CHT acts to increase the minimum temperature at the stagnation region for all metals that are used in the simulation. The minimum temperature increases with the metal thermal conductivity (Al & Cu), where the maximum convective heat transfer is taken place. The disc thickness effect on the T_{min} is more apparent for the metal with lower thermal conductivity (316SST) as shown in Figure 7. This completely agrees with the results discussed for q_{T0} in Figure 6. The q_{T0} will not change significantly with Cu metal. This will act to maintain T_{min} nearly constant for Cu as disc thickness increases. However, there is noticeable increase in q_{T0} for Al as shown in Figure 6, which acts to increase T_{min} for Al as disc thickness increases.

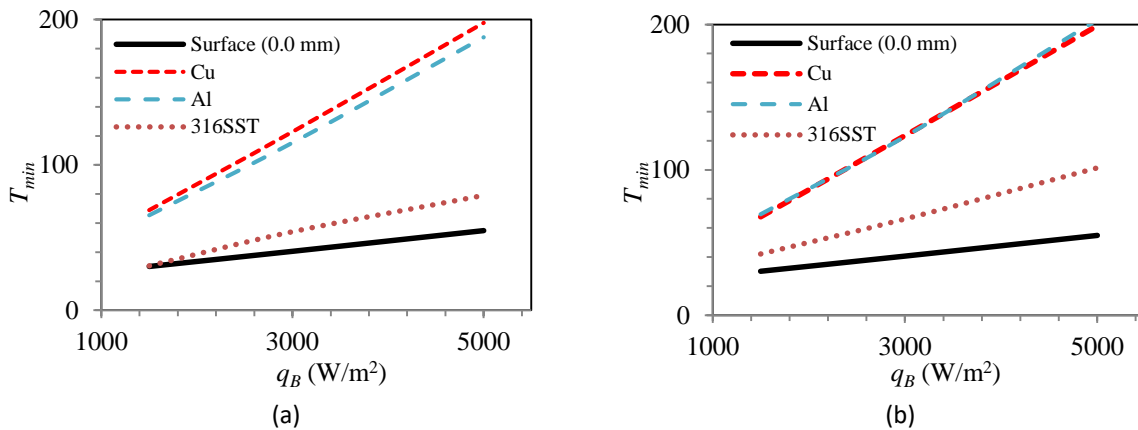


Fig. 7. The effect of the CHT process on disc minimum temperature (a) disc $t_p = 5.0$ mm, (b) disc $t_p = 10.0$ mm

5. Conclusions

A numerical CFD study has been carried out to evaluate the CHT effect on the thermal characteristics of the air jet impingement process. The cases are simulated using STAR-CCM+ - Siemens PLM commercial code with an unstructured polyhedral mesh. The effect of boundary heat flux and the target thickness on the thermal characteristics were investigated in this study. The following results are the main conclusions from the current study

- i. The CHT process is governed by both components of the metal thermal resistance, i.e., the radial and axial thermal resistance of the target.
- ii. The metal type has a significant effect on the CHT process. The Nu/Nu_0 profile is shifted downwards from the one with no CHT as the thermal conductivity of the metal increases.
- iii. For a given boundary heat flux, the stagnation region Nusselt number (Nu_0) decreases as the thermal conductivity of the metal increases. The decrease in the Nu_0 is more obvious at higher heat fluxes. The Nu_0 value for all metals becomes comparable as thermal boundary heat flux approaches zero.
- iv. The CHT process enhances the local convective heat transfer at fluid-solid interface up to a certain radial extent from the stagnation region compared to the process with no CHT. For a given thickness, the extent of heat transfer enhancements depends on the thermal conductivity of the metal.
- v. At the stagnation region, the thickness is more dominant than thermal conductivity on thermal characteristics for metal with low thermal conductivity. Contrary to this, thermal conductivity is more dominant than the thickness on thermal characteristics for metal with high thermal conductivity. The influence of the thickness becomes negligible when the thermal conductivity of the metal approaches infinity.
- vi. The CHT process acts to increase the minimum temperature at the stagnation region. For a given thickness, the temperature increases with the metal thermal conductivity, while for a given thermal conductivity, the temperature of the stagnation region increases with the thickness.

Acknowledgment

This research was made possible by the facilities of the Shared Hierarchical Academic Computing Network (SHARCNET: www.sharcnet.ca) and Compute/Calcul Canada.

References

- [1] Nasif, G., R. M. Barron, and R. Balachandar. "Simulation of jet impingement heat transfer onto a moving disc." *International Journal of Heat and Mass Transfer* 80 (2015): 539-550. <https://doi.org/10.1016/j.ijheatmasstransfer.2014.09.036>
- [2] Nasif, G., R. M. Barron, and R. Balachandar. "Numerical simulation of piston cooling with oil jet impingement." *Journal of Heat Transfer* 138, no. 12 (2016). <https://doi.org/10.1115/1.4034162>
- [3] Nasif, Ghassan Gus. "CFD Simulation of Oil Jets with Application to Piston Cooling." University of Windsor (2014).
- [4] Stevens, J., and Brent W. Webb. "Local heat transfer coefficients under an axisymmetric, single-phase liquid jet." (1991): 71-78. <https://doi.org/10.1115/1.2910554>
- [5] Lee, Jungho Lee, Sang-Joon. "Stagnation region heat transfer of a turbulent axisymmetric jet impingement." *Experimental Heat Transfer* 12, no. 2 (1999): 137-156. <https://doi.org/10.1080/089161599269753>
- [6] Liu, Xin, L. A. Gabour, and J. H. Lienhard. "Stagnation-point heat transfer during impingement of laminar liquid jets: analysis including surface tension." *Journal of Heat Transfer* 115, no. 1 (1993): 99-105. <https://doi.org/10.1115/1.2910677>
- [7] Haidar, Chadia, Rachid Boutarfa, and Souad Harmand. "Numerical and Experimental Study of Convective Heat Exchanges on a Rotating Disk with an Eccentric Impinging Jet." *Journal of Advanced Research in Fluid Mechanics and Thermal Sciences* 57, no. 2 (2019): 208-215.
- [8] Aroonrujiphan, Chattawat, and Chayut Nuntadusit. "Flow and Heat Transfer Characteristics of Impinging Bubbly Jet." *Journal of Advanced Research in Fluid Mechanics and Thermal Sciences* 74, no. 1 (2020): 68-80. <https://doi.org/10.37934/arfmts.74.1.6880>
- [9] Zhu, Xiao Wei, Lei Zhu, and Jing Quan Zhao. "An in-depth analysis of conjugate heat transfer process of impingement jet." *International Journal of Heat and Mass Transfer* 104 (2017): 1259-1267. <https://doi.org/10.1016/j.ijheatmasstransfer.2016.09.075>

- [10] Bouafia, Islam, Razli Mehdaoui, Syham Kadri, and Mohammed Elmir. "Conjugate Natural Convection in a Square Porous Cavity Filled with a Nanofluid in the Presence of Two Isothermal Cylindrical Sources." *Journal of Advanced Research in Fluid Mechanics and Thermal Sciences* 80, no. 1 (2021): 147-164. <https://doi.org/10.37934/arfmts.80.1.147164>
- [11] Mensch, Amy, and Karen A. Thole. "Conjugate heat transfer analysis of the effects of impingement channel height for a turbine blade endwall." *International Journal of Heat and Mass Transfer* 82 (2015): 66-77. <https://doi.org/10.1016/j.ijheatmasstransfer.2014.10.076>
- [12] Hussein, Ahmed Kadhim, Muhaiman Alawi Mahdi, and Obai Younis. "Numerical Simulation of Entropy Generation of Conjugate Heat Transfer in A Porous Cavity with Finite Walls and Localized Heat Source." *Journal of Advanced Research in Fluid Mechanics and Thermal Sciences* 84, no. 2 (2021): 116-151. <https://doi.org/10.37934/arfmts.84.2.116151>
- [13] Pozzi, Amilcare, and Renato Tognaccini. "Time singularities in conjugated thermo-fluid-dynamic phenomena." *Journal of Fluid Mechanics* 538 (2005): 361-376. <https://doi.org/10.1017/S002211200500529X>
- [14] Pozzi, Amilcare, and Renato Tognaccini. "Coupling of conduction and convection past an impulsively started semi-infinite flat plate." *International journal of heat and mass transfer* 43, no. 7 (2000): 1121-1131. [https://doi.org/10.1016/S0017-9310\(99\)00210-0](https://doi.org/10.1016/S0017-9310(99)00210-0)
- [15] Fourcher, B., and K. Mansouri. "An approximate analytical solution to the Graetz problem with periodic inlet temperature." *International journal of heat and fluid flow* 18, no. 2 (1997): 229-235. [https://doi.org/10.1016/S0142-727X\(96\)00089-6](https://doi.org/10.1016/S0142-727X(96)00089-6)
- [16] Radenac, Emmanuel, Jérémie Gressier, and Pierre Millan. "Methodology of numerical coupling for transient conjugate heat transfer." *Computers & Fluids* 100 (2014): 95-107. <https://doi.org/10.1016/j.compfluid.2014.05.006>
- [17] Sosnowski, Marcin, Jaroslaw Krzywanski, Karolina Grabowska, and Renata Gnatowska. "Polyhedral meshing in numerical analysis of conjugate heat transfer." In *EPJ Web of Conferences*, vol. 180, p. 02096. EDP Sciences, 2018. <https://doi.org/10.1051/epiconf/201817002096>
- [18] Versteeg, Henk Kaarle, and Weeratunge Malalasekera. *An introduction to computational fluid dynamics: the finite volume method*. Pearson education, 2007.
- [19] Ge, Shemin. "A governing equation for fluid flow in rough fractures." *Water Resources Research* 33, no. 1 (1997): 53-61. <https://doi.org/10.1029/96WR02588>
- [20] Nasif, G., R. Balachandar, and R. M. Barron. "Mean characteristics of fluid structures in shallow-wake flows." *International Journal of Multiphase Flow* 82 (2016): 74-85. <https://doi.org/10.1016/j.ijmultiphaseflow.2016.03.001>